ACS Photonics

Article

pubs.acs.org/journal/apchd5

Loss-Mitigated Collective Resonances in Gain-Assisted Plasmonic Mesocapsules

Melissa Infusino,*[,†,‡] Antonio De Luca,[†,§] Alessandro Veltri,[†,§] Carmen Vázquez-Vázquez,[⊥] Miguel A. Correa-Duarte,[⊥] Rakesh Dhama,[§] and Giuseppe Strangi*[,‡]

[†]CNR-IPCF UOS di Cosenza, Licryl Laboratory, and [‡]Department of Physics, Case Western Reserve University, 10600 Euclid Avenue, Cleveland, United States

[§]Department of Physics, University of Calabria, 87036 Rende, Italy

[⊥]Department of Physical Chemistry, University of Vigo, 36310 Vigo, Spain

Supporting Information

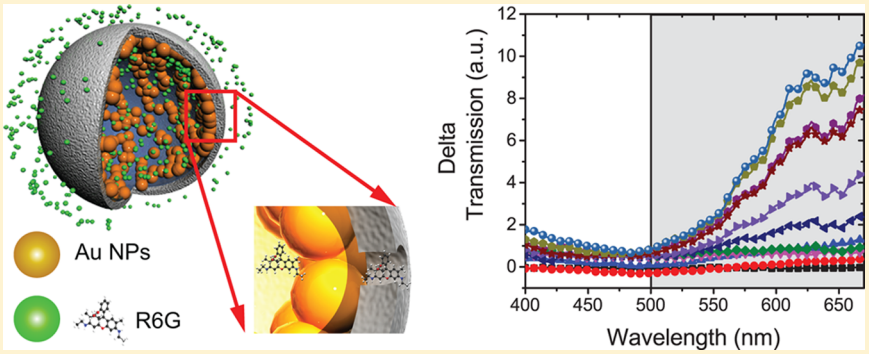

ABSTRACT: Inherent optical losses of plasmonic materials represent a crucial issue for optoplasmonics, whereas the realization of hierarchical plasmonic nanostructures implemented with gain functionalities is a promising and valuable solution to the problem. Here we demonstrate that porous silica capsules embedding gold nanoparticles (Au NPs) and fabricated at a scale intermediate between the single plasmonic nanostructure and bulk materials show remarkable form−function relations. At this scale, in fact, the plasmon−gain interplay is dominated by the location of the gain medium with respect to the spatial distribution of the local field. In particular, the hollow spherical cavities of these structures allow regions of uniform plasmonic field where the energy transfer occurring between chromophoric donors and the surrounding plasmonic acceptors gives rise to a broadband attenuation of losses.

KEYWORDS: *active plasmonics, loss compensation, nanostructured systems, collective resonances, pump−probe spectroscopy*

Plasmon physics deals with coherent plasma oscillations of metal free electrons, which, under specific excitation conditions, provide a fascinating scientific scenario of resonances and interplay at the nanoscale level. In particular, during the past decade, optoplasmonics proved to be a very promising cross-disciplinary research area from both scientific and technological viewpoints. Optoplasmonic properties arise in metal nanostructures because of a controlled shaping of the local electromagnetic fields and giant plasmon resonances occurring at scales that are much shorter than visible wavelengths. These resonances in hybrid (metal−dielectric−chromophores) nanostructures result in strong multipolar couplings at the nano-object scale, giving rise to metal enhancement effects in the designed materials. Indeed, their remarkable optical responses allow the coherent generation of light,[1−5] the selective sensing of organic and biological markers with very high resolution,[6,7] and imaging at subwavelength scale by beating the diffraction limit.[8−10] Nanoplasmonics has received a drastically strong boost by the recent development of sophisticated characterization techniques and the great advancement of fabrication methods based on nanochemistry routes and assemblies.[11−18] However, the crucial point of the metal-based plasmonic materials remains the intrinsic optical losses located at the resonance frequencies. In fact, the strong radiation damping at visible wavelengths leads to the shadowing of their extraordinary electromagnetic properties. Gain-enhanced materials are a potential solution to this problem,[19−26] but the conception of realistic three-dimensional designs is still a challenging task.

The idea is to optimize plasmon−gain dynamics so that coherent and nonradiative energy transfer processes between excitonic states (chromophore-donor) and plasmon states (metal-acceptor) can effectively occur. Programming this interplay by controlling the dominant parameters of plasmon−gain interaction provides a powerful tool to trigger

Received: December 27, 2013
Published: March 26, 2014

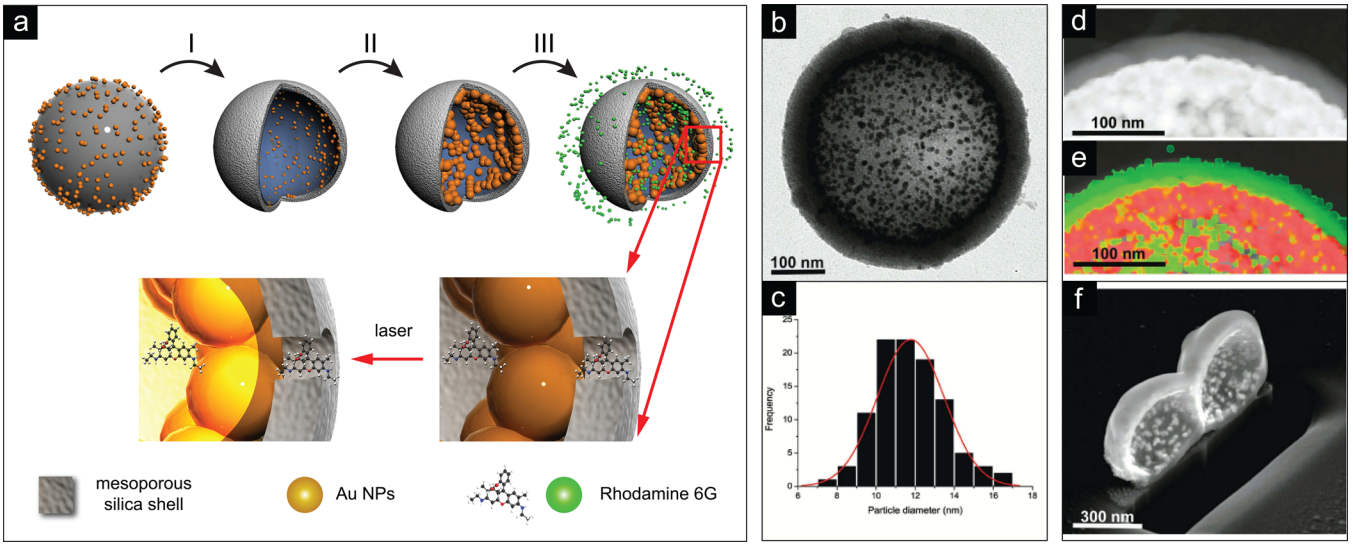

Figure 1. (a) Schematic of the synthesis of plasmonic mesocapsules. (b) TEM image of a typical plasmonic mesocapsule. (c) Statistical distribution of Au NP diameters, with an average of 11.5 ± 1.7 nm. (d) STEM and (e) combined XEDS elemental mapping images from the same mesocapsule, Au = red and SiO_2 = green. (f) FIB cross-section image.

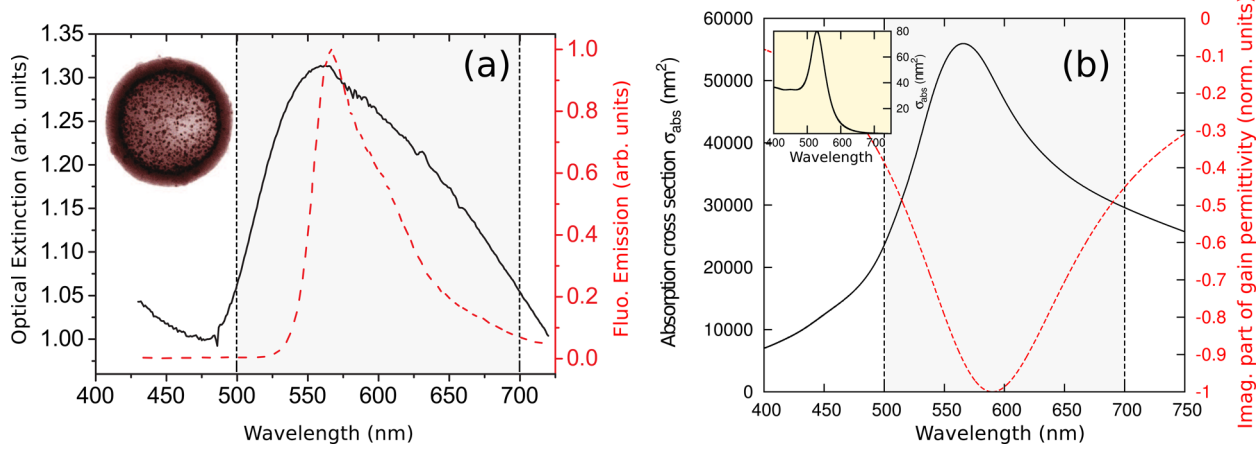

Figure 2. (a) Mesocapsule plasmonic resonance (black continuous line) and R6G emission spectrum (red dashed line). (b) Calculated absorption cross section (black continuous line) and imaginary part of gain permittivity (red dashed line). In the inset we show the absorption cross section of a single metal nanoparticle.

relevant physical effects: optical loss compensation, superabsorption, enhanced photoluminescence, surface-enhanced Raman scattering, and laser action.

In this paper we report on the loss mitigation observed in a dispersion of porous silica mesocapsules embedding plasmonic nanoparticles (NPs) in a gain-doped solution. These plasmonic mesocapsules, obtained via colloid chemistry routes, show a broad plasmon resonance band covering a large portion of the visible spectrum (500−700 nm). In particular, we discuss several decisive experiments that demonstrate a substantial gain-induced broadband loss mitigation. In previous works based on the study of gold nanospheres functionalized with gain[27−29] selective optical loss mitigation has been observed. In that case, although optical losses were efficiently attenuated, this was restricted to a narrow spectral range. The present work shows the first experimental evidence of optical loss mitigation in a template embedding plasmonic nanoparticles and involving a large portion of the visible spectrum; it represents therefore a step forward in the direction of bulk plasmonic materials.

RESULTS AND DISCUSSION

We have designed and fabricated plasmonic structures, with a diameter of 530 nm, resembling a reverse bumpy ball configuration in which multiple Au NPs are grafted on the inner walls of porous silica capsules (Figure 1a). Their fabrication procedure, shown schematically in Figure 1a, is based on previous synthetic developments,[30,31] whose details are reported in the Methods section.

Figure 1b shows the typical transmission electron microscope (TEM) image of a plasmonic mesocapsule; the Au NPs supported on the inner wall of the porous silica shell are clearly visible as dark spots. Figure 1c shows the statistical distribution of Au NP diameters, the average diameter is 11.5 ± 1.7 nm. The spatial distribution of the Au NP growth at the inner wall of the silica shell is clearly evidenced by the focused ion beam (FIB) cross-section analysis of a typical plasmonic capsule (Figure 1f). Scanning transmission electron microscopy (STEM) in Figure 1d and X-ray energy dispersive spectroscopy (XEDS) in Figure 1e provide further evidence about the

dx.doi.org/10.1021/ph400174p | ACS Photonics 2014, 1, 371−376

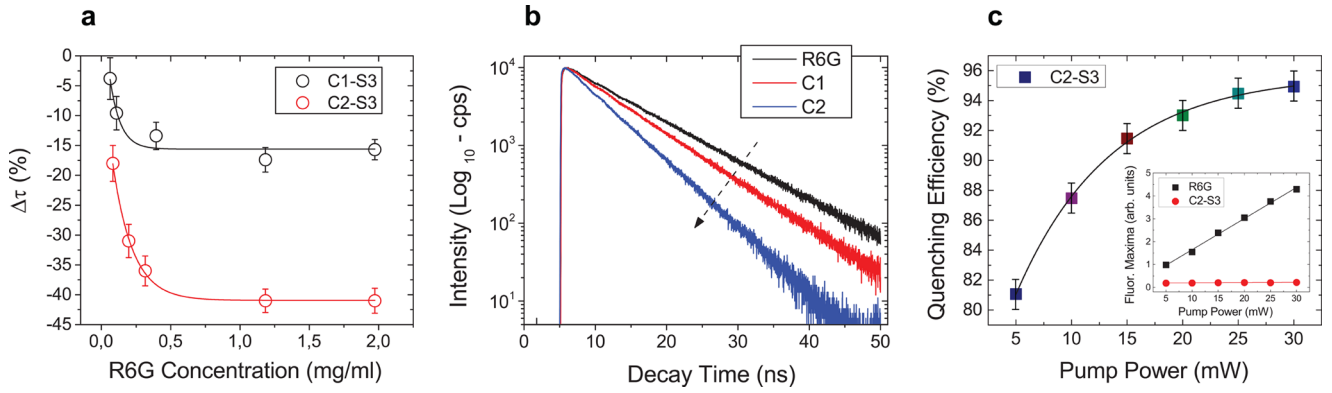

Figure 3. (a) Percentage decrease of the fluorescence decay time vs dye concentration for two different concentrations of mesocapsules (C1 = 1.25 mg mL^{-1}; C2 = 7.5 mg mL^{-1}). (b) Decay time data for pure R6G at a concentration Cr = 1.2 mg mL^{-1} in ethanol (black line) and for two mesocapsule dispersions at concentrations C1 (red line) and C2 (blue line) in an R6G solution (Cr = 1.2 mg mL^{-1}). (c) Fluorescence quenching efficiency as a function of the pump energy; in the inset we show the fluorescence maxima of R6G at a concentration Cr = 1.2 mg mL^{-1} in ethanol (black squares) and the fluorescence maxima for an isoconcentrated solution of R6G to which we added mesocapsules (7.5 mg mL^{-1}) (red dots). The fluorescence quenching efficiency has been calculated by using the data in the inset.

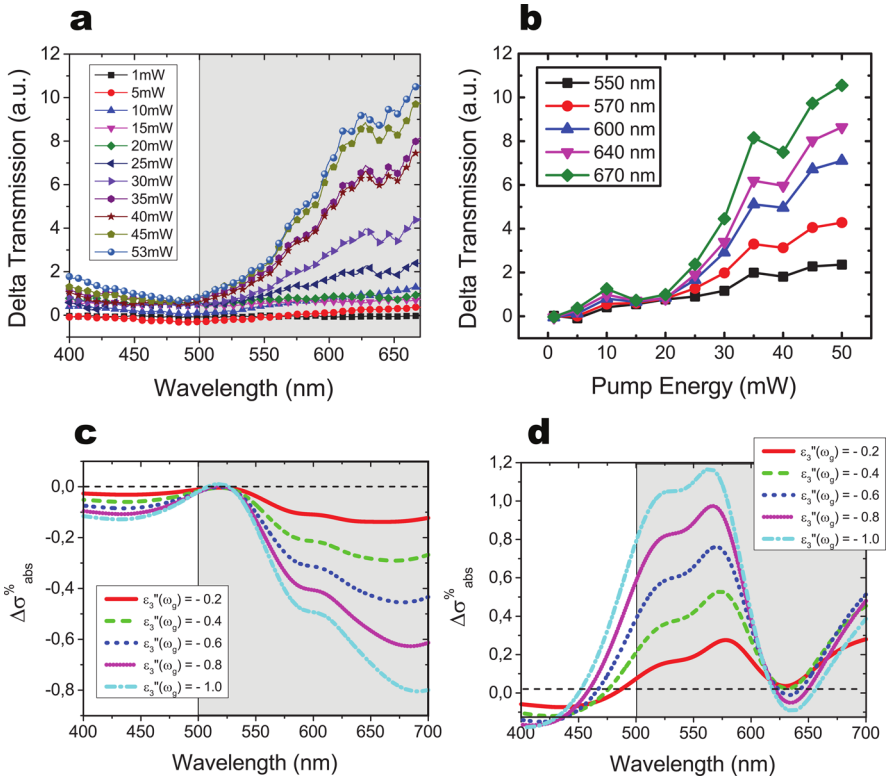

Figure 4. Measured percentage change of the light probe that is transmitted (a) by the mesocapsule gain assisted system as a function of pump energy. (b) Cuts of the previous curves for five different wavelengths of transmitted intensity as a function of pump energy. Calculated behavior for $\Delta\sigma^{\%}_{abs}$ for different value levels of gain $\varepsilon_3''(\omega_g)$ from −0.2 to −1.0). (c) Gain elements are assumed to be both outside and in the core of the mesocapsules. (d) Gain elements are assumed to be only outside the core of mesocapsules.

homogeneous nature of the silica shell; moreover no trace of gold is detected on its outer surface.

Noteworthy is the plasmonic band resulting from the nanoparticles' arrangement, which produces a spectrally wider and red-shifted resonance compared to that of the single metal nanoparticle (see Figure 2a,b). It is, in fact, known that nanoresonators, which alone would produce a specific plasmon resonance, when in close proximity mix and hybridize, creating a completely different response. This effect can be treated just like electron wave functions of atomic and molecular orbitals.[32,33] In this paper we want to underline how the mesocapsules can be considered a loss-compensation model system in between a single nanoresonator and a bulk material. For this reason, we theoretically describe the hybridization with a simpler, yet geometrically sound approach[34] by means of a homogenization rule widely used to calculate the collective optical properties of bulk materials.

Nanoporous silica was chosen for the dielectric shell because it is a largely used host material for encapsulating dyes or drugs by means of a simple impregnation approach.[35,36] The pores (2−5 nm in diameter) of the silica shell have been loaded with rhodamine 6G (R6G) as the gain material by soaking the

dx.doi.org/10.1021/ph400174p | ACS Photonics 2014, 1, 371−376

plasmonic mesostructures in an ethanolic R6G solution (step III and zoom in Figure 1a; see details in the Supporting Information). In previous studies, dealing with the effect of isolated metallic nanoparticles on the fluorophores' spontaneous emission rate has demonstrated that the nonradiative energy transfer processes are largely dependent on distance, with a maximum located where the plasmonic field is more intense, namely, at a few nanometers from the nanoparticle surface.[37−41] In the case of plasmonic mesocapsules, the impregnation of the hollow cores with the gain solution, as we will discuss in the following, is very effective for the promotion of nonradiative coupling. R6G has been chosen because its emission spectrum overlaps the mesocapsule plasmonic band (Figure 2a), matching the resonant energy transfer condition.

The decreasing of the fluorophores' spontaneous emission lifetime in the presence of a plasmonic resonator is a signature effect of the nonradiative resonant energy transfer[39,42,43] (see Figure 3a,b). Consequently, in order to identify the optimal ratio between fluorophore and mesocapsule concentrations, a series of fluorescence lifetime measurements have been carried out. They show a maximum reduction of the decay time of 41.0 ± 2.6% (Figure 3a,b); therefore we used the corresponding concentrations (C1 = 7.5 mg mL^{-1} for mesocapsules and Cr = 1.2 mg mL^{-1} for R6G) in all the subsequent experiments. The decay time data for the dye concentration Cr for both mesocapsule concentrations C1 and C2 are shown in Figure 3b. In Figure 3c we report the fluorescence quenching efficiency, calculated as $Q = 1 - (F/F_0)$, where F and F_0 are the fluorescence signal intensity in the presence and in the absence of mesocapsules, as a function of the pump power. The nonlinear increasing of Q as a function of the pump power can be ascribed to the resonant energy transfer processes occurring between plasmonic mesocapsules and dye molecules. If the two media were uncoupled, the mesocapsules would have acted like static quenchers and the quenching rate would have been constant. Eventually fluorescence spectroscopy gives us the clear proof of a resonant energy transfer between gain and plasmonic medium; in order to demonstrate that this coupling is actually working as a loss-compensating mechanism, an ultrafast pump−probe experiment for the simultaneous measure of Rayleigh scattering and transmission has been set up. According to the Beer−Lambert−Bouguer law, by measuring simultaneously Rayleigh scattering and transmission either in the absence or in the presence of a pump, we are able to understand if the absorptive power of the material is affected by the gain presence. The experimental details are described in the Methods section; moreover a sketch of the experimental setup for both pump−probe and fluorescence experiments is reported in the Supporting Information. While the scattering intensity of the probe beam seems to be unaffected by excitation energy, a broadband enhancement of the transmitted light through the sample has been measured (see Figure 4a). It shows a typical threshold value for the average pump power (about 20 mW), above which we observe a superlinear increase of the transmission. In fact, the transmitted probe light increases an order of magnitude with respect to the absence of the exciting field (pump pulses).

Figure 4b shows delta transmission, evaluated as $(I_p - I_0)/I_0$, where I_p and I_0 are the intensities of the probe light in the presence and in the absence of a pump, as a function of the pump power.

To support the experimental results, we realized an analytical model based on Mie theory and used the steady-state solution of the Maxwell−Bloch equations (i.e., a Lorentzian line shape) to describe the gain behavior. This approach has the advantage of being geometrically solid, which is of primary importance considering the specificity of the described structures, and it has been proved to provide an accurate description of the interplay between gain and plasmonic nano-objects, when, as in our case, the gain level is lower than the one needed to push the system into an amplifying, unstable regime[44] (details in the Supporting Information). In particular, the mesocapsule has been modeled as a core/shell system in which the permittivity of the shell made of mesoporous silica encapsulating gold nanoparticles is calculated as an effective medium via the Maxwell Garnett mixing rule. The result of our calculations shows that, if the presence of gain elements is supposed to be only outside the gold-rich inner shell (namely, diluted in ethanol or impregnated in the outer porous shell), no loss-mitigation effects occur (see Figure 4d). In particular, the model predicts an increasing of the absorption cross-section in a spectral range below 550 nm and a reduction (even negative values) between 550 and 600 nm. On the other hand, if the gain is infiltrated in the hollow core, the absorption cross-section is broadband reduced (negative values), corresponding to a loss mitigation on a large spectral region (see Figure 4c).

In Figure 4c,d $\Delta\sigma^{\%}_{abs} = (\sigma_{abs}(\varepsilon_3'') - \sigma^0_{abs})/\sigma^0_{abs}$ is presented as a function of different gain level (ε_3''). Here σ^0_{abs} represents the absorption cross-section in the absence of gain.[45] This result is not surprising because, in the hollow core of the mesocapsule, the electric field is spatially uniform and, consequently, the coupling is highly efficient for all the gain molecules present in this region, thus allowing for an effective loss mitigation. From these results, one can infer that, in the experiments, a non-negligible amount of gain molecules infiltrated the hollow core of the mesocapsules, emphasizing how important it is to strategically position the gain with respect to the geometry of the plasmonic structure. We evaluated that the density of dye molecules inside the mesocapsule cavity has to be comparable to the density of dye molecules outside; so by considering the concentration used in the experiments we estimated that the number of dye molecules contained in each capsule is about 10^5.

Furthermore, it is known that the orientation of the dipole momentum of the gain elements plays a fundamental role in the optimization of the energy exchange.[46] As a consequence, with the gain elements present in our system dispersed in a solution, their dipole momenta are free to reorient according to the electric field, even inside the mesostructures. This makes these systems much more efficient for loss-mitigation purposes than functionalized nanostructures in which the gain elements are embedded with random orientation within a solid dielectric host.

CONCLUSIONS

In summary, we have described a broadband plasmonic response strongly coupled with a gain medium located right at the heart of hierarchically complex plasmonic mesocapsules. Colloid chemistry proved to be an unparalleled method to devise a perfect morphological definition of the capsules having gold nanoparticles grafted on the inner walls, leading to a remarkable plasmon hybridization effect. This artificial supra-metamolecular organization showed striking opto-plasmonic features. In particular, gold nanoparticles' surface plasmon states overcame a hybridization process, resulting in a broadband plasmon (>200 nm) acting as a hole acceptor for

the nonradiative excitation energy channel of the chromophores. Not unexpectedly, both measurements and theory confirm a remarkable process of optical loss mitigation. Hybridized plasmons strongly coupled to gain elements represent novel quantum nanophotonic systems, which could enable a massive advancement toward semitransparent metallodielectric photonic metamaterials, biosensors, and nanolasers.

METHODS

Polystyrene (PS) beads of 530 nm were functionalized by using the layer-by-layer assembly technique (LbL),[30,47,48] resulting in an ordered multilayer composed of four monolayers of polyelectrolyte (PS/PSS/PAH/PSS/PAH), where PAH stands for poly(allylamine hydrochloride) (M_w 56 000) and PSS for poly(sodium styrenesulfonate) (M_w 70 000). This polyelectrolyte film provides the PS particles with the necessary electrostatic functionality for the adsorption of gold seeds. The gold seeds (1−3 nm; [Au] = 10^{-3} M) were synthesized as described elsewhere.[30,49] In this case, 10 mL of functionalized PS beads (2.5 mg mL^{-1}) was added dropwise to 50 mL of Au seed solution under sonication. The resultant solution was left to stand for 2 h. The excess of gold seeds not deposited on the PS surface was removed by three centrifugation−redispersion cycles with pure water (5000 rpm, 20 min). The final redispersion was in 5 mL of an 1:1 ethanol/water mixture.

In order to carry out the mesoporous silica coating, the method described by Yonghui Deng et al.[50] was partially followed. Briefly, the previous PS@Au-seed suspension, 5 mg mL^{-1}, was added drop by drop under sonication to a mixed solution of cetyl trimethylammonium bromide (CTAB) (200 mg), deionized water (80 mL), ammonia aqueous solution (28 wt %, 0.730 mL), and ethanol (60 mL). The resultant solution was homogenized by sonication for 20 min. Then, 2 mL of a 5% (v/v) solution of tetraethoxysilane (TEOS) in ethanol was added dropwise to the previous suspension under sonication. This mixture was stirred for 2 days in order to have a homogeneous silica growth. Then it was centrifuged three times and washed with water. Polystyrene and CTAB templates were removed by calcination at 550 °C for 20 h. A solution of gold prereduced Au^+ was prepared as described elsewhere.[51] A first growth of gold seeds inside the mesoporous capsules was achieved by adding 57 mL of Au^+ solution and 170 μL of formaldehyde solution (37 wt %) to 10 mL, 2.5 mg mL^{-1} of Au-seeds@SiO_2 mesoporous-h under vigorous stirring. After 5 min of reaction, the color of the solution changed from red to purple-blue and 15 min later from purple-blue to gray-blue. The sample was centrifuged three times and washed with water. A second growth was carried out just by adding 40 mL of Au^+ solution and 90 μL of formaldehyde to a volume of 5 mL, 2.5 mg mL^{-1} of the previous solution. After 30 min of vigorous stirring, the sample was cleaned by three centrifugation−redispersion cycles with pure water. The final redispersion of the capsules after the first and second growth was in ethanol. To investigate the modification of sample absorbance, we used an ultrafast spectroscopic pump−probe setup (for details see the Supporting Informations). Samples were excited at 375 nm by means of a Ti:sapphire pulsed laser (repetition rate = 80 MHz, pulse width = 140 fs, by Coherent Inc.) coupled to a second harmonic generator (SHG) module. The probe beam was a supercontinuum light generated by using the Ti:sapphire source this time coupled to a nonlinear photonic crystal fiber. For fluorescence spectroscopy measurements (both steady state and time-correlated single photon counting investigations) the excitation at 375 nm was produced by using the Ti:sapphire laser coupled to the SHG module and to a pulse picker used to decrease the repetition rate in the range between 4 and 5 MHz. This arrangement allows the beam to be synchronized with a multipronged spectrofluorometer used for detecting fluorescence light.

ASSOCIATED CONTENT

Supporting Information

The optical setup used for fluorescence spectroscopy and pump−probe experiments and the theoretical model are described with more detail in the Supporting Information file. This material is available free of charge via the Internet at http://pubs.acs.org.

AUTHOR INFORMATION

Corresponding Authors

*E-mail: mxi98@case.edu.
*E-mail: gxs284@case.edu.

Notes

The authors declare no competing financial interest.

ACKNOWLEDGMENTS

G.S. acknowledges support of the Ohio Third Frontier Project Research Cluster on Surfaces in Advanced Materials (RC-SAM). The research leading to these results has received funding from the European Union's Seventh Framework Programme ([FP7/2008]) Metachem Project under grant agreement no. 228762 and from the Calabria Region (ROP) ESF-2007/2013 IV Axis Human Capital-Operative Objective M2-Action D.5.

REFERENCES

(1) Oulton, R. F.; Sorger, V. J.; Zentgraf, T.; Ma, R.; Gladden, C.; Dai, L.; Bartal, G.; Zhang, X. Plasmon Lasers at Deep Subwavelength Scale. *Nature* **2009**, *461*, 629−632.

(2) Sorger, V. J.; Oulton, R. F.; Yao, J.; Bartal, G.; Zhang, X. Plasmonic Fabry-Pérot Nanocavity. *Nano Lett.* **2009**, *9*, 3489−3493.

(3) Sorger, V. J.; Oulton, R. F.; Yao, J.; Bartal, G.; Zhang, X. Spotlight on Plasmon Lasers. *Science* **2011**, *333*, 709−710.

(4) Berini, P.; De Leon, I. Surface Plasmon-Polariton Amplifiers and Lasers. *Nat. Photonics* **2012**, *6*, 16−24.

(5) Gordon, J.; Ziolkowski, R. W. The Design and Simulated Performance of a Coated Nano-particle Laser. *Opt. Express* **2007**, *15*, 2622−2653.

(6) Anker, J. N.; Hall, W. P.; Lyandres, O.; Shah, N. C.; Zhao, J.; Duyne, R. P. V. Biosensing with Plasmonic Nanosensors. *Nat. Mater.* **2008**, *7*, 442−453.

(7) Steward, M. E.; Anderton, C. R.; Thompson, L.; Maria, J.; Gray, S. K.; Rogers, J. A.; Nuzzo, R. G. Nanostructured Plasmonic Sensors. *Chem. Rev.* **2008**, *108*, 494−521.

(8) Pendry, J. B. Negative Refraction Makes a Perfect Lens. *Phys. Rev. Lett.* **2000**, *85*, 3966−3969.

(9) Zhang, X.; Liu, Z. Superlenses to Overcome the Diffraction Limit. *Nat. Mater.* **2008**, *7*, 435−441.

(10) Ishii, S.; Shalaev, V. M.; Kildishev, A. V. Holey-Metal Lenses: Sieving Single Modes with Proper Phases. *Nano Lett.* **2013**, *13*, 159−163.

(11) Malassis, L.; Massé, P.; Tréguer-Delapierre, M.; Mornet, S.; Weisbecker, P.; Barois, P.; Simovski, C. R.; Kravets, V. G.; Grigorenko, A. N. Topological Darkness in Self-Assembled Plasmonic Metamaterials. *Adv. Mater.* **2013**, *26*, 324−330.

(12) Ji, Q.; Acharya, S.; Richards, G. J.; Zhang, S.; Vieaud, J.; Hill, J. P.; Ariga, K. Alkyl Imidazolium Ionic-Liquid-Mediated Formation of Gold Particle Superstructures. *Langmuir* **2013**, *29*, 7186−7194.

(13) Dintinger, J.; Mühlig, S.; Rockstuhl, C.; Scharf, T. A Bottom-up Approach to Fabricate Optical Metamaterials by Self-Assembled Metallic Nanoparticles. *Opt. Mater. Express* **2012**, *2*, 269−278.
(14) Simon, U. Nanoparticle Self-Assembly: Bonding Them All. *Nat. Mater.* **2013**, *12*, 694−696.
(15) Blum, A. S.; Soto, C. M.; Wilson, C. D.; Cole, J. D.; Kim, M.; Gnade, B.; Chatterji, A.; Ochoa, W. F.; Lin, T.; Johnson, J. E.; Ratna, B. R. Cowpea Mosaic Virus as a Scaffold for 3-D Patterning of Gold Nanoparticles. *Nano Lett.* **2004**, *4*, 867−870.
(16) Coursault, D.; Grand, J.; Zappone, B.; Ayeb, H.; Lévi, G.; Félidj, N.; Lacaze, E. Linear Self-Assembly of Nanoparticles within Liquid Crystal Defect Arrays. *Adv. Mater.* **2012**, *24*, 1461−1465.
(17) Sashuk, V.; Winkler, K.; Áżywociński, A.; Wojciechowski, T.; Górecka, E.; Fiałkowski, M. Nanoparticles in a Capillary Trap: Dynamic Self-Assembly at Fluid Interfaces. *ACS Nano* **2013**, *7*, 8833−8839.
(18) Dintinger, J.; Tang, B.-J.; Zeng, X.; Liu, F.; Kienzler, T.; Mehl, G. H.; Ungar, G.; Rockstuhl, C.; Scharf, T. A Self-Organized Anisotropic Liquid-Crystal Plasmonic Metamaterial. *Adv. Mater.* **2013**, *25*, 1999−2004.
(19) Noginov, M. A.; Zhu, G.; Bahoura, M.; Adegoke, J.; Small, C. E.; Ritzo, B. A.; Drachev, V. P.; Shalaev, V. M. Enhancement of Surface Plasmons in an Ag Aggregate by Optical Gain in a Dielectric Medium. *Opt. Lett.* **2006**, *31*, 3022−3024.
(20) Noginov, M. A.; Podolskiy, V. A.; Zhu, G.; Mayy, M.; Bahoura, M.; Adegoke, J.; Ritzo, B. A.; Reynolds, K. Compensation of Loss in Propagating Surface Plasmon Polariton by Gain in Adjacent Dielectric Medium. *Opt. Express* **2008**, *16*, 1385−1392.
(21) Stockman, M. I. Spaser Action, Loss Compensation, and Stability in Plasmonic Systems with Gain. *Phys. Rev. Lett.* **2011**, *106*, 156802.
(22) Stockman, M. I. Loss Compensation by Gain and Spasing. *Philos. Trans. R. Soc. A* **2011**, *369*, 3510−3524.
(23) Soukoulis, C. M.; Wegener, M. Optical Metamaterials—More Bulky and Less Lossy. *Science* **2010**, *330*, 1633−1634.
(24) Campione, S.; Albani, M.; Capolino, F. Complex Modes and Near-zero Permittivity in 3D Arrays of Plasmonic Nanoshells: Loss Compensation Using Gain. *Opt. Mater. Express* **2011**, *1*, 1077−1089.
(25) Campione, S.; Capolino, F. Composite Material Made of Plasmonic Nanoshells with Quantum Dot Cores: Loss-Compensation and ε-near-Zero Physical Properties. *Nanotechnology* **2012**, *23*, 235703−235708.
(26) Hess, O.; Pendry, J.; Maier, S. A.; Oulton, R. F.; Hamm, J.; Tsakmakidis, K. L. Active Nanoplasmonic Metamaterials. *Nat. Mater.* **2012**, *11*, 573−584.
(27) Strangi, G.; De Luca, A.; Ravaine, S.; Ferrie, M.; Bartolino, R. Gain Induced Optical Transparency in Metamaterials. *Appl. Phys. Lett.* **2011**, *98*, 251912.
(28) De Luca, A.; Grzelczak, M. P.; Pastoriza-Santos, I.; Liz-Marzán, L. M.; Deda, M. L.; Striccoli, M.; Strangi, G. Dispersed and Encapsulated Gain Medium in Plasmonic Nanoparticles: a Multi-pronged Approach to Mitigate Optical Losses. *ACS Nano* **2011**, *5*, 5823−5829.
(29) De Luca, A.; Ferrie, M.; Ravaine, S.; La Deda, M.; Infusino, M.; Rahimi Rashed, A.; Veltri, A.; Aradian, A.; Scaramuzza, N.; Strangi, G. Gain Functionalized Core-Shell Nanoparticles: The Way to Selectively Compensate Absorptive Losses. *J. Mater. Chem.* **2012**, *22*, 8846−8852.
(30) Sanlés-Sobrido, M.; Exner, W.; Rodríguez-Lorenzo, L.; Rodríguez-González, B.; Correa-Duarte, M. A.; Alvarez-Puebla, R. A.; Liz-Marzán, L. Design of SERS-Encoded, Submicron, Hollow Particles through Confined Growth of Encapsulated Metal Nanoparticles. *J. Am. Chem. Soc.* **2009**, *131*, 2699−2705.
(31) Sanlés-Sobrido, M.; Pérez-Lorenzo, M.; Rodríguez-González, B.; Salgueiriño, V.; Correa-Duarte, M. A. Highly Active Nanoreactors: Nanomaterial Encapsulation Based on Confined Catalysis. *Angew. Chem., Int. Ed.* **2012**, *51*, 3877−3882.
(32) Prodan, E.; Radloff, C.; Halas, N. J.; Nordlander, P. A Hybridization Model for the Plasmon Response of Complex Structures. *Science* **2003**, *302*, 419−422.
(33) Halas, N. J.; Lal, S.; Chang, W.; Link, S.; Nordlander, P. Plasmons in Strongly Coupled Metallic Nanostructures. *Chem. Rev.* **2011**, *111*, 3913−3961.
(34) Baudrion, A.-L.; Perron, A.; Veltri, A.; Bouhelier, A.; Adam, P.-M.; Bachelot, R. Reversible Strong Coupling in Silver Nanoparticle Arrays Using Photochromic Molecules. *Nano Lett.* **2013**, *13*, 282−286.
(35) Suh, M.; Lee, H.-J.; Park, J.-Y.; Lee, U.-H.; Kwon, Y.-U.; Kim, D. J. A Mesoporous Silica Thin Film as Uptake Host for Guest Molecules with Retarded Release Kinetics. *ChemPhysChem* **2008**, *9*, 1402−1408.
(36) Wang, L.; Liu, Y.; Chen, F.; Zhang, J.; Anpo, M. Manipulating Energy Transfer Processes between Rhodamine 6G and Rhodamine B in Different Mesoporous Hosts. *J. Phys. Chem. C* **2007**, *111*, 5541−5548.
(37) Yun, C. S.; Javier, A.; Jennings, T.; Fisher, M.; Hira, S.; Peterson, S.; Hopkins, B.; Reich, N. O.; Strouse, G. F. Nanometal Surface Energy Transfer in Optical Rulers, Breaking the FRET Barrier. *J. Am. Chem. Soc.* **2005**, *127*, 3115−3119.
(38) Anger, P.; Bharadwaj, P.; Novotny, L. Enhancement and Quenching of Single-Molecule Fluorescence. *Phys. Rev. Lett.* **2006**, *96*, 113002.
(39) Peng, B.; Zhang, Q.; Liu, X.; Ji, Y.; Demir, H.; Huan, C. H. A.; Sum, T. C.; Xiong, Q. Fluorophore-Doped Core-Multishell Spherical Plasmonic Nanocavities: Resonant Energy Transfer toward a Loss Compensation. *ACS Nano* **2012**, *6* (7), 6250−6259.
(40) Tovmachenko, O. G.; Graf, C.; van den Heuvel, D. J.; van Blaaderen, A.; Gerritsen, H. C. Fluorescence Enhancement by Metal-Core/Silica-Shell Nanoparticles. *Adv. Mater.* **2006**, *18*, 91−95.
(41) Viste, P.; Plain, J.; Jaffiol, R.; Vial, A.; Adam, P.-M.; Royer, P. Enhancement and Quenching Regimes in Metal-Semiconductor Hybrid Optical Nanosources. *ACS Nano* **2010**, *4*, 759−764.
(42) Dulkeith, E.; Morteani, A. C.; Niedereichholz, T.; Klar, T. A.; Feldmann, J.; Levi, S. A.; van Veggel, F. C. J. M.; Reinhoudt, D. N.; Moller, M.; Gittins, D. I. Fluorescence Quenching of Dye Molecules near Gold Nanoparticles: Radiative and Nonradiative Effects. *Phys. Rev. Lett.* **2002**, *89*, 203002.
(43) Bhowmick, S.; Saini, S.; Shenoy, V. B.; Bagchi, B. Resonance Energy Transfer from a Fluorescent Dye to a Metal Nanoparticle. *J. Chem. Phys.* **2006**, *125*, 181102/1−6.
(44) Veltri, A.; Aradian, A.; Chipouline, A. Time-Dynamical Model for the Optical Response of a Plasmonic Nanoparticle Immersed in an Active Gain Medium. Submitted.
(45) Veltri, A.; Aradian, A. Optical Response of a Metallic Nanoparticle Immersed in a Medium with Optical Gain. *Phys. Rev. B* **2012**, *85*, 1−5.
(46) Lakowicz, J. R. *Principles of Fluorescence Spectroscopy*, 3rd ed.; Springer: New York, 2006; Chapter XIII, p 444.
(47) Shchukin, D. G.; Radtchenko, I. L.; Sukhorukov, G. B. Micron-Scale Hollow Polyelectrolyte Capsules with Nanosized Magnetic Fe_3O_4 Inside. *Mater. Lett.* **2003**, *57*, 1743−1747.
(48) Vázquez-Vázquez, C.; Salgueiriño, V.; Correa-Duarte, M.; Pérez-Lorenzo, M. Fabricación de Cápsulas Inorgánicas: Introducción Experimental al Desarrollo de Estructuras Nanométricas Funcionales. *An. Quím.* **2012**, *108*, 1−6.
(49) Duff, D. G.; Baiker, A.; Edwards, P. P. A New Hydrosol of Gold Clusters. 1. Formation and Particle Size Variation. *Langmuir* **1993**, *9*, 2301−2309.
(50) Deng, Y.; Qi, D.; Deng, C.; Zhang, X.; Zhao, D. Superparamagnetic High-Magnetization Microspheres with an Fe_3O_4@SiO_2 Core and Perpendicularly Aligned Mesoporous SiO_2 Shell for Removal of Microcystins. *J. Am. Chem. Soc.* **2008**, *130*, 28−29.
(51) Pham, T.; Jackson, J. B.; Halas, N. J.; Lee, T. R. Preparation and Characterization of Gold Nanoshells Coated with Self-Assembled Monolayers. *Langmuir* **2002**, *18*, 4915−4920.